

Post-Newtonian Dynamics in Dense Star Clusters: Highly-Eccentric, Highly-Spinning, and Repeated Binary Black Hole Mergers

Carl L. Rodriguez,¹ Pau Amaro-Seoane,² Sourav Chatterjee,³ and Frederic A. Rasio³

¹*MIT-Kavli Institute for Astrophysics and Space Research,
77 Massachusetts Avenue, 37-664H, Cambridge, MA 02139, USA*

²*Institute of Space Sciences (ICE, CSIC) & Institut d'Estudis Espacials de Catalunya (IEEC)
at Campus UAB, Carrer de Can Magrans s/n 08193 Barcelona, Spain*

*Institute of Applied Mathematics, Academy of Mathematics and Systems Science, CAS, Beijing 100190, China
Kavli Institute for Astronomy and Astrophysics, Beijing 100871, China*

Zentrum für Astronomie und Astrophysik, TU Berlin, Hardenbergstraße 36, 10623 Berlin, Germany

³*Center for Interdisciplinary Exploration and Research in Astrophysics (CIERA) and Dept. of Physics and Astronomy,
Northwestern University, 2145 Sheridan Rd, Evanston, IL 60208, USA*

(Dated: December 15, 2017)

We present models of realistic globular clusters with post-Newtonian dynamics for black holes. By modeling the relativistic accelerations and gravitational-wave emission in isolated binaries and during three- and four-body encounters, we find that nearly half of all binary black hole mergers occur inside the cluster, with about 10% of those mergers entering the LIGO/Virgo band with eccentricities greater than 0.1. In-cluster mergers lead to the birth of a second generation of black holes with larger masses and high spins, which, depending on the black hole natal spins, can sometimes be retained in the cluster and merge again. As a result, globular clusters can produce merging binaries with detectable spins *regardless* of the birth spins of black holes formed from massive stars. These second-generation black holes would also populate any upper mass gap created by pair-instability supernovae.

I. INTRODUCTION

With the recent detections of five binary black hole (BBH) mergers, and one binary neutron star merger, the era of gravitational wave (GW) astrophysics has arrived at last [1–5]. Despite significant theoretical work, the origins of these systems, particularly the heavier BBHs, remain an open question. Both stellar evolution in isolated massive binaries [e.g. 6–10] and dynamical formation in dense star clusters [e.g. 11–22] have been shown to produce merging BBHs similar to GW150914 [23, 24]. Understanding which formation pathways are at play will be critical for the interpretation of GW data. While many signatures of dynamical assembly have been proposed, such as highly-eccentric mergers occurring in strong chaotic encounters [25] or anti-alignment of the BH spins with the orbit [26], none of the BBH mergers detected so far by LIGO/Virgo have displayed any of those signatures clearly [see 27].

What *has* been displayed clearly in each BBH merger is the birth of a new rapidly-spinning BH with a mass (almost) equal to the sum of its progenitor masses. Many of these new BHs, particularly the remnants of GW150914, GW170104, and GW170814, are significantly more massive than what is thought to form during the collapse of a single star, where the pair-instability mechanism limits the remnant BH mass to $\lesssim 50M_{\odot}$ [28]. Were one of these mergers to occur in a dense star cluster, however, the merger product could easily exchange into another BBH and merge again. Because of the distinct BH masses and spins in such second-generation (2G) mergers, it has been suggested that such a population could be easily identifiable with future LIGO/Virgo detections

[29, 30].

In this letter, we present the first models of realistic globular clusters (GCs) with fully post-Newtonian (pN) stellar dynamics. While relativistic N -body dynamics has been studied previously for highly idealized systems [e.g., 31–40] or open clusters [e.g., 22], we show here for the first time using self-consistent dynamical models of massive GCs that pN effects play a key role in assembling dynamically the merging BBHs detectable by LIGO/Virgo. In our new pN models, we observe that roughly half of all BBH mergers occur inside clusters, with a significant fraction of those ($\sim 10\%$) merging with eccentricities greater than 0.1 following GW captures. In-cluster mergers produce a second generation of BHs that, if not ejected from the cluster through GW recoil, will dynamically exchange into new binaries only to merge again. These 2G BBH mergers have components with large spins and masses significantly beyond what is possible from the collapse of a single star; they may be quite common, with as many as $\sim 20\%$ of BBH mergers from our models having components formed in a previous merger.

Throughout this paper, we assume a flat Λ CDM cosmology with $h = 0.679$ and $\Omega_M = 0.3065$ [41].

II. POST-NEWTONIAN DYNAMICS

We have computed the new GC models presented here using the **Cluster Monte Carlo** (CMC) code. CMC has been developed over many years [42, 43], and includes all the necessary physics for the long-term evolution of GCs, including two-body relaxation [44, 45], single and binary

stellar evolution [46–48], galactic tides, three-body binary formation [49], and three- and four-body gravitational encounters via the `fewbody` package [50, 51]. We have shown in [52] that CMC can reproduce with a high degree of fidelity both the global cluster properties and BBH distributions computed with state-of-the-art direct N -body simulations [53], while at the same time being at least two orders of magnitude faster (essential for the sort of extensive parameter-space study presented here). Furthermore, CMC has been upgraded [21] to employ the most recent prescriptions for stellar-wind-driven mass loss [54, 55] and compact-object formation [56], allowing us to compare our results directly to those of population synthesis studies for isolated binaries [e.g. 23].

To incorporate pN effects into CMC, we make the following modifications. We account for relativistic effects during three- and four-body encounters by adopting a modified version of the `fewbody` code with pN accelerations up to and including the 2.5pN order. This code has been described in detail in [27, 57] and has been shown to conserve energy to 2pN order and to reproduce the inspiral times for compact binaries [58]. For BBHs which merge during an encounter, we perform a standard sticky-sphere merger, using detailed, spin-dependent fitting formulas from analytic and numerical relativity calculations [59–72]. See Appendix A for details. For BBHs which do not merge during a `fewbody` encounter, we directly integrate the orbit-averaged Peters equations [58] for the change in semi-major axis and eccentricity due to GW emission. See Appendix A. This represents a departure from our previous work where we relied on the binary stellar evolution module [BSE, 47], which, by default, only considers GW emission for binaries whose semi-major axis is less than $10R_{\odot}$. We initially assume all BHs from stellar collapse have no spins at birth ($\chi_b = 0$, where χ is the dimensionless Kerr spin parameter), though we relax this assumption in Section V.

We generate 24 GC models covering a range of masses, metallicities, galactocentric distances, and virial radii, similar to those observed in the Milky Way and beyond. These initial conditions are identical to those from [21], allowing us to explicitly compare our pN results to those in the literature. Our physics for single and binary stellar evolution is nearly identical to [21]. We have added a prescription for stellar mass loss via pulsational-pair-instability supernovae and stellar destruction via pair-instability supernovae. This physics, powered by the rapid production of electron-positron pairs in the stellar core [28], places a well-understood upper limit on the masses of BHs that can form from the collapse of a single star. We take the limit from [73] of $\sim 45M_{\odot}$ which is reduced to $\sim 40M_{\odot}$ via neutrino emission. See Appendix B for details. This limit is in tentative agreement with the BH mass distribution measured by LIGO/Virgo [74]. In our simulations, no BH can be born with a mass above $40M_{\odot}$ unless the BH or its stellar progenitor has undergone a dynamical merger or mass transfer. Finally, unlike previous studies [20, 52, 75], we have not

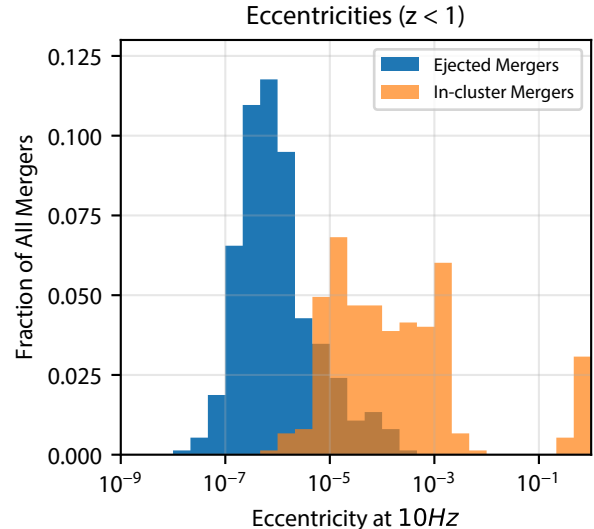


FIG. 1. The eccentricities of BBHs from the 24 GC models that merge at low redshifts. We calculate the eccentricity when the BBH enters the LIGO/Virgo detection band at a (circular) GW frequency of 10Hz. The distribution is clearly trimodal: the first peak corresponds to BBHs which merge after ejection from the cluster [similar to 21, Figure 10]. The second peak corresponds to BBH mergers which occur in the cluster. The final peak, at $e > 0.1$, corresponds to in-cluster mergers which occur during a strong encounter, when the BBH enters the LIGO/Virgo band during a GW capture. Note that the two distributions are normalized to the total number of mergers (in-cluster and ejected).

weighted our models according to the distribution of observed GCs. We will explore more realistic sets of models in future work focusing specifically on LIGO/Virgo detection rates. In practice a more realistic weighting should make little difference, as our previously adopted weighting scheme primarily selected BBHs from the most massive clusters, which also contribute the majority of sources in our current grid.

III. IN-CLUSTER MERGERS

With the addition of the pN physics, we see a significant increase in the number of in-cluster mergers. Whereas before the number of in-cluster mergers was a minor correction to the BBH mergers in the local universe [0.06% of mergers at $z < 1$, see 21], we now find that *nearly half* of mergers now occur inside the cluster. For the 24 models considered here we find a total of 2819 mergers, 55% of which occur in the cluster. At low redshifts ($z < 1$), this number decreases to 45%, as the primordial binaries which merged at early times after a common-envelope phase have merged many Gyr ago. Compared to similar models without pN physics [21], the number of ejected BBH mergers at $z < 1$ de-

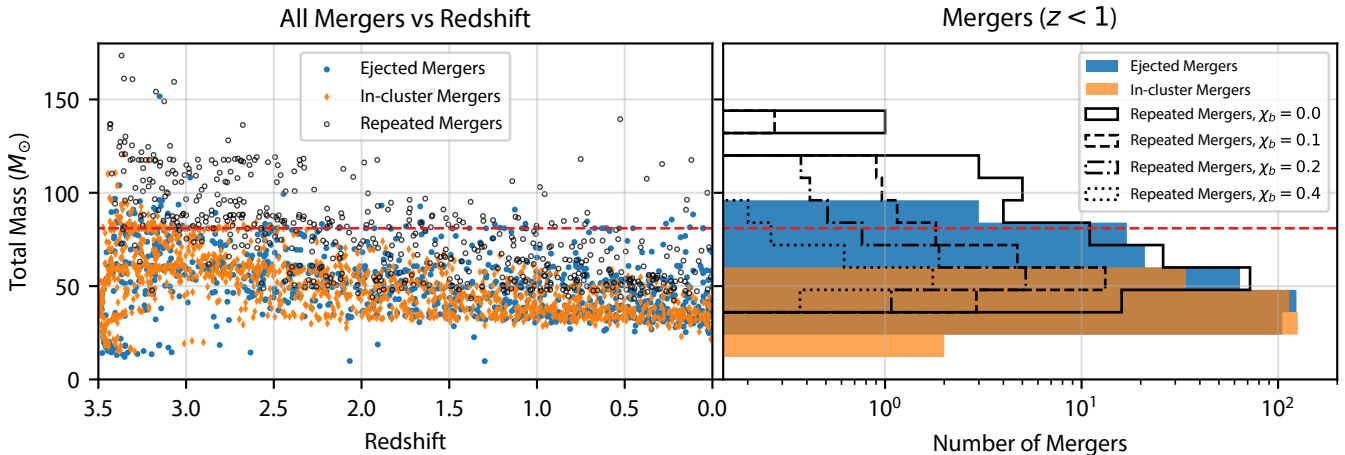


FIG. 2. The total mass of merging BBHs from all 24 GC models. On the **left**, we show all mergers as a function of redshift, with the orange diamonds and blue points showing in-cluster and ejected mergers, respectively. The black circles show 2G mergers (both in-cluster and ejected) which have at least one component that was formed from a previous BBH merger. The **right** panel shows the mass distribution of these mergers at low redshifts ($z < 1$). As the spins are increased from $\chi_b = 0$ to $\chi_b = 0.4$, the number of 2G mergers decreases significantly, as their progenitors were less likely to be retained in the cluster. See the discussion in Section V. The red-dashed line indicates the maximum mass of first-generation BBHs ($\sim 81M_{\odot}$) with our assumed pair-instability supernova limit. The handful of first-generation BBHs which merge above this are the result of either stable mass transfer or stellar collisions prior to BH formation.

creases by $\sim 20\%$ (496 versus 410). However, the number of in-cluster mergers has jumped significantly, from one to 338. This increases the total number of mergers (in-cluster and ejected) by $\sim 50\%$.

In Figure 1, we show the eccentricity distribution of merging binaries as they enter the LIGO/Virgo band (which we define as a circular GW frequency of 10Hz). We see a clear separation in eccentricity between BBHs which merge in the cluster and those that merge after being ejected from the cluster. For the in-cluster mergers, we also find a clear bimodality, with the lower peak corresponding to isolated binaries that merge after a dynamical encounter and the higher peak ($e > 0.1$) corresponding to sources which merge *during* the encounter via GW capture. Although previous work [25, 27, 76] has shown through scattering experiments that such mergers are to be expected at the 1% level, this is the first work to show that these mergers occur in realistic GC environments. From our combined 24 models, we find that about 10% of the in-cluster mergers ($\sim 4\%$ of all mergers) at $z < 1$ occur during these GW captures, in good agreement with analytic work [77].

IV. MERGERS OVER COSMIC TIME

In Figure 2, we show the mergers of BBHs as a function of cosmological redshift. After mass segregation (~ 1 Gyr), the most massive BHs have migrated to the cluster center, where the density of objects is high enough to enable the formation of BBHs via three-body encounters [e.g., 14, 78]. Once a BBH has formed, it will continue

to undergo scattering three- and four-body encounters with nearby stars and BHs, characteristically shrinking the semi-major axis of the binary with each interaction [79]. This “hardening” process continues until either the binary is ejected from the cluster by the third body or until GWs drive the binary to merger.

What is immediately striking in Figure 2 is that the mass distributions for in-cluster and ejected binaries are significantly different at low redshifts. This arises from the delay times between formation and mergers for ejected BBHs. When a BBH is ejected from the cluster, it may still take several Gyr to merge in the field [see e.g., 80, and references therein]. Even for the most massive clusters, the median inspiral time for ejected binaries is ~ 10 Gyr [e.g., 21, Figure 1]. In effect, the ejected BBHs which merge today drew their components from the *initial* distribution of BH masses in the cluster, where the masses varied from $5M_{\odot}$ to $40M_{\odot}$. On the other hand, the in-cluster mergers have effectively no delay time, and their components are drawn from the *present-day* distribution of BH masses in the cluster. Because old GCs have ejected their most-massive BHs many Gyrs ago [78], the BBHs merging in the cluster today are typically lower-mass than those that were ejected many Gyr ago.

Another interesting feature of Figure 2 is the presence of BBH mergers in the upper-mass gap, beyond the mass limit imposed by pair-instability supernovae. The increased number of in-cluster mergers allows the GCs to produce significant number of 2G BBH mergers, some of which will have components above the maximum mass for BHs born from a single stellar collapse. As these systems can only be produced through multiple mergers, they will

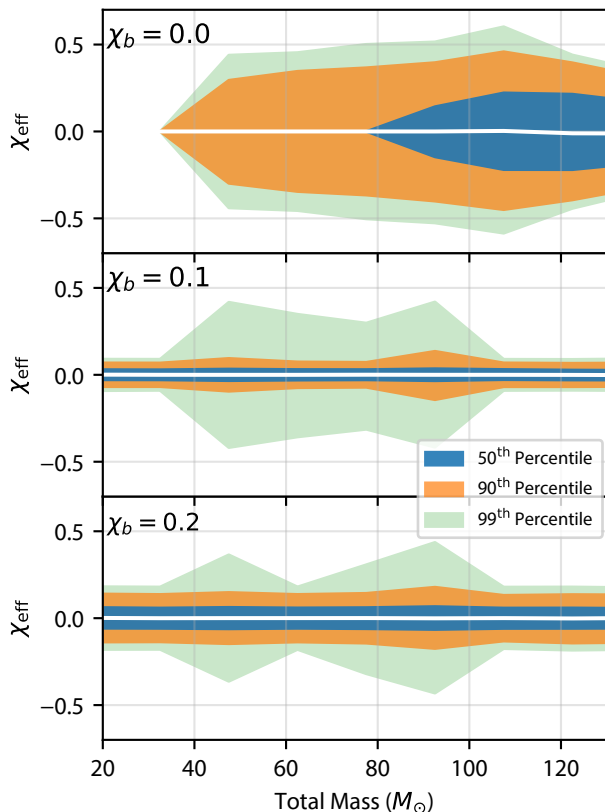


FIG. 3. The distributions of χ_{eff} from BBHs that merge at $z < 1$, divided into bins of $15M_{\odot}$. Each bin shows the median (white line), 50th, 90th, and 99th percentiles of χ_{eff} for all BBH mergers with that mass. For each binary, we average over $N = 10^3$ random spin orientations. For the 2G mergers, we use $N = 10^3$ times the probability of each component having been retained in the cluster following its earlier mergers (see discussion in Section V). As the birth spins (χ_b) of the BHs are increased, fraction of 2G BBHs retained in the cluster decreases; however, the overall magnitudes of χ_{eff} increases, as the first generation of BBHs begin to produce mergers with measurable spins.

immediately be identifiable as having arisen from a dynamical environment. The rate of such mergers is small, but LIGO/Virgo is more sensitive to mergers with more massive components [the detection horizon scales with the mass of the more massive component as $m^{2.2}$, 74]. At the expected sensitivity for Advanced LIGO’s third observing run [81], a BBH with component masses of $40M_{\odot} + 80M_{\odot}$ could be detected out to $z \sim 1$, encompassing a comoving volume of space three times larger than was observed during LIGO’s second science run [82].

V. BLACK HOLE SPIN AND RECOIL KICKS

As a conservative assumption, we have assumed that all BHs in the cluster are born with no intrinsic spin. This

is consistent with all but one [GW151226, 5] of the BBHs detected by LIGO/Virgo so far. However, the presence of high BH spins, suggested by observations of BH X-ray binaries [see 83, for a review], can radically change the results presented here: depending on the spin magnitudes and orientations, merging BBHs can get kicks as high as 4000 km/s [e.g., 84], significantly larger than the escape speed of a typical GC. As a result, the 2G mergers shown in the left-hand panel of Figure 2 would not have formed if BHs are born with large spins, since their components would not have been retained in the cluster [14].

We can estimate how the numbers in Figure 2 would have changed under different assumptions for BH birth spins. For each repeated merger, we calculate the probability that each of the components would have been retained in the cluster given different birth spins. This is done by computing the recoil kicks over 1000 realizations of the spin orientations at merger. The probability of retaining each progenitor is simply the fraction of mergers for which the recoil speed is smaller than the cluster escape speed where the merger occurred. For each 2G BBH merger, we take the product of the retention probabilities for each component as the probability of that 2G merger occurring. We show the retention of these BBHs in the right panel of Figure 2 by weighting each 2G BBH merger by its retention probability. As expected, the number of 2G BBH mergers decreases as the birth spins of the BHs are increased. When $\chi_b = 0$, we find that $\sim 20\%$ of mergers at $z < 1$ are 2G mergers. As the spins are increased, this number decreases, and once $\chi_b = 0.4$, we observe $\mathcal{O}(1)$ 2G mergers, compared to the 672 first-generation mergers which occur at $z < 1$.

These assumption have significant implications for the measurable spins of BBH mergers. As shown by numerical relativity [85] and idealized pN N -body simulations with spins [40], repeated mergers of BBHs in clusters with near-equal masses will tend to produce BHs with $\chi \sim 0.7$. But what LIGO/Virgo is most sensitive to is not the spin magnitudes of the BBHs components [86], but the effective spin of the BBH, defined as the mass-weighted projection of the two spins onto the orbital angular momentum:

$$\chi_{\text{eff}} \equiv \left[\frac{m_1 \vec{\chi}_1 + m_2 \vec{\chi}_2}{m_1 + m_2} \right] \cdot \hat{L}, \quad (1)$$

where \hat{L} is the direction of the orbital angular momentum and $\vec{\chi}_{1,2}$ are the dimensionless-spin vectors for the BHs. For dynamically-formed binaries, the isotropic distribution of the orbit and spin vectors means that (1) will be peaked at $\chi_{\text{eff}} = 0$ with symmetric tails whose extend depends on the BH spin magnitudes. We show the distributions of χ_{eff} in Figure 3. When the initial BH spins are low, the 2G systems are the only BBHs which merge with observably large spins. The fraction of systems with large spins increases as a function of total mass, since these larger systems (particularly those beyond the pulsational-pair instability limit) are predom-

inantly formed through repeated mergers. As the birth spins are increased, the number of 2G mergers (with their characteristically large spins) decreases as their components are more likely to be ejected from the cluster during their first merger. But the total number of BBH systems with non-zero χ_{eff} increases, as the first generation of BHs will now form mergers with observable spins. This result is key: one of the most promising ways for identifying a dynamically-formed BBH merger is by the alignment of the spins, with anti-aligned systems ($\chi_{\text{eff}} < 0$) being a clear indicator of dynamical formation [24]. These results indicate that dynamical assembly in dense star clusters will inevitably produce a merger with $\chi_{\text{eff}} < 0$, regardless of the BH birth spins.

VI. CONCLUSION

We have shown that the inclusion of pN effects can have significant implications for BBH mergers from dense star clusters detectable by LIGO/Virgo. By accounting for GW emission from isolated binaries and during three- and four-body dynamical encounters, we find that a significant number of mergers occur in the cluster, and that about 4% of all mergers (and $\sim 10\%$ of in-cluster mergers) in our models will enter the LIGO/Virgo detection band with high residual eccentricity ($e > 0.1$). Because of

this, GCs can potentially produce a significant number of 2G BBH mergers with detectable spins and with masses larger than those produced through the collapse of single stars. Dynamics in dense star clusters can therefore produce BBH mergers with anti-aligned spins (a clear indicator of a dynamical origin) *regardless of the initial spins of first-generation BHs*: if natal BH spins are large, then GCs can produce BBH mergers with $\chi_{\text{eff}} < 0$ from first-generation systems. If the spins are initially small [as predicted by e.g., 27], then the BBH merger products can often be retained in the cluster, forming a second generation of BBHs with large spins ($\chi \sim 0.7$).

We thank Carl-Johan Haster, Michael Zevin, Johan Samsing, Davide Gerosa, Salvatore Vitale, Chris Pankow, and Scott Hughes for useful discussions. CR is supported by a Pappalardo Postdoctoral Fellowship at MIT. This work was supported by NASA Grant NNX14AP92G and NSF Grant AST-1716762 at Northwestern University. PAS acknowledges support from the Ramón y Cajal Programme of the Ministry of Economy, Industry and Competitiveness of Spain, the COST Action GWverse CA16104, and the CAS President's International Fellowship Initiative. CR thanks the Niels Bohr Institute for its hospitality while part of this work was completed, and the Kavli Foundation and the DNRF for supporting the 2017 Kavli Summer Program. CR and FR also acknowledge support from NSF Grant PHY-1607611 to the Aspen Center for Physics, where this work was started.

-
- [1] B. P. Abbott, R. Abbott, T. D. Abbott, F. Acernese, K. Ackley, C. Adams, T. Adams, P. Addesso, R. X. Adhikari, V. B. Adya, et al., *Physical Review Letters* **119**, 1 (2017).
 - [2] B. P. Abbott, R. Abbott, T. D. Abbott, F. Acernese, K. Ackley, C. Adams, T. Adams, P. Addesso, R. X. Adhikari, V. B. Adya, et al., *Physical Review Letters* **118**, 221101 (2017).
 - [3] B. P. Abbott, R. Abbott, T. D. Abbott, F. Acernese, K. Ackley, C. Adams, T. Adams, P. Addesso, R. X. Adhikari, V. B. Adya, et al., *Physical Review Letters* **119**, 30 (2017).
 - [4] B. P. Abbott, R. Abbott, T. D. Abbott, M. R. Abernathy, F. Acernese, K. Ackley, C. Adams, T. Adams, P. Addesso, R. X. Adhikari, et al., *Physical Review Letters* **116**, 061102 (2016).
 - [5] B. P. Abbott, R. Abbott, T. D. Abbott, M. R. Abernathy, F. Acernese, K. Ackley, C. Adams, T. Adams, P. Addesso, R. X. Adhikari, et al., *Physical Review Letters* **116**, 241103 (2016).
 - [6] K. Belczynski, M. Dominik, T. Bulik, R. OShaughnessy, C. Fryer, and D. E. Holz, *The Astrophysical Journal* **715**, L138 (2010).
 - [7] P. Marchant, N. Langer, P. Podsiadlowski, T. M. Tauris, and T. J. Moriya, *Astronomy & Astrophysics* **588**, A50 (2016).
 - [8] P. Podsiadlowski, S. Rappaport, and Z. Han, *Mon. Not. R. Astron. Soc* **341**, 385 (2003).
 - [9] I. Mandel and S. E. De Mink, *MNRAS* **458**, 2634 (2016).
 - [10] S. E. De Mink and I. Mandel, *Mon. Not. R. Astron. Soc* **460**, 3545 (2016).
 - [11] S. Sigurdsson and L. Hernquist, *Nature* **364**, 423 (1993).
 - [12] S. F. Portegies Zwart and S. L. W. Mcmillan, *The Astrophysical Journal* **528**, 17 (2000).
 - [13] R. M. OLeary, F. A. Rasio, J. M. Fregeau, N. Ivanova, and R. OShaughnessy, *The Astrophysical Journal* **637**, 937 (2006).
 - [14] M. C. Miller and V. M. Lauburg, *The Astrophysical Journal* **692**, 917 (2009), 0804.2783.
 - [15] J. M. B. Downing, M. J. Benacquista, M. Giersz, and R. Spurzem, *Mon. Not. R. Astron. Soc* **407**, 1946 (2010).
 - [16] S. Banerjee, H. Baumgardt, and P. Kroupa, *Mon. Not. R. Astron. Soc* **402**, 371 (2010).
 - [17] J. M. B. Downing, M. J. Benacquista, M. Giersz, and R. Spurzem, *Mon. Not. R. Astron. Soc* **407**, 133 (2011).
 - [18] Y.-B. Bae, C. Kim, and H. M. Lee, *Mon. Not. R. Astron. Soc* **440**, 2714 (2014).
 - [19] B. M. Ziosi, M. Mapelli, M. Branchesi, and G. Tormen, *Mon. Not. R. Astron. Soc* **441**, 3703 (2014).
 - [20] C. L. Rodriguez, M. Morscher, B. Pattabiraman, S. Chatterjee, C.-J. Haster, and F. A. Rasio, *Physical Review Letters* **115**, 051101 (2015).
 - [21] C. L. Rodriguez, S. Chatterjee, and F. A. Rasio, *Physical Review D* **93**, 084029 (2016).
 - [22] S. Banerjee, *Mon. Not. R. Astron. Soc* **467**, 524 (2017).
 - [23] K. Belczynski, D. E. Holz, T. Bulik, and R. OShaughnessy, *Nature* **534**, 512 (2016).
 - [24] C. L. Rodriguez, M. Zevin, C. Pankow, V. Kalogera, and

- F. A. Rasio, *The Astrophysical Journal* **832**, L2 (2016).
- [25] J. Samsing, M. MacLeod, and E. Ramirez-Ruiz, *The Astrophysical Journal* **784**, 71 (2014).
- [26] C. Rodriguez, M. Morscher, B. Pattabiraman, S. Chatterjee, C.-J. Haster, and F. Rasio, *Physical Review Letters* **116** (2016).
- [27] P. Amaro-Seoane and X. Chen, *Mon. Not. R. Astron. Soc* **458**, 3075 (2016), 1512.04897.
- [28] S. E. Woosley, *The Astrophysical Journal* **836**, 244 (2016).
- [29] M. Fishbach, D. E. Holz, and B. Farr, *The Astrophysical Journal* **840**, L24 (2017).
- [30] D. Gerosa and E. Berti, *Physical Review D* **95**, 124046 (2017).
- [31] M. H. Lee, *Astrophys J* v418 **418**, 147 (1993).
- [32] M. H. Lee, Ph.D. Thesis (1992).
- [33] S. L. Shapiro and S. A. Teukolsky, *Astrophys J* **298**, 34 (1985).
- [34] S. L. Shapiro and S. A. Teukolsky, *Astrophys J* **292**, L41 (1985).
- [35] F. A. Rasio, S. L. Shapiro, and S. A. Teukolsky, *Astrophys J* **336**, L63 (1989).
- [36] G. D. Quinlan and S. L. Shapiro, *Astrophys J* **321**, 199 (1987).
- [37] G. D. Quinlan and S. L. Shapiro, *Astrophys J* **343**, 725 (1989).
- [38] G. D. Quinlan and S. L. Shapiro, *Astrophys J* **356**, 483 (1990).
- [39] G. Kuper, P. Amaro-Seoane, and R. Spurzem, *Mon. Not. R. Astron. Soc* **371**, L77 (2006), astro-ph/0602125.
- [40] P. Brem, P. Amaro-Seoane, and R. Spurzem, *Mon. Not. R. Astron. Soc* **434**, 2999 (2013), 1302.3135.
- [41] Planck Collaboration, P. A. R. Ade, N. Aghanim, M. Arnaud, M. Ashdown, J. Aumont, C. Baccigalupi, A. J. Banday, R. B. Barreiro, J. G. Bartlett, et al. (2015).
- [42] K. J. Joshi, F. A. Rasio, S. P. Zwart, and S. Portegies Zwart, *The Astrophysical Journal* **540**, 969 (2000).
- [43] B. Pattabiraman, S. Umbreit, W.-k. Liao, A. Choudhary, V. Kalogera, G. Memik, and F. A. Rasio, *The Astrophysical Journal Supplement Series* **204**, 15 (2013).
- [44] M. Hénon, *Astrophysics and Space Science* **14**, 151 (1971).
- [45] M. Henon, *Astrophysics and Space Science* **13**, 284 (1971).
- [46] J. R. Hurley, O. R. Pols, and C. A. Tout, *Mon. Not. R. Astron. Soc* **315**, 543 (2000).
- [47] J. R. Hurley, C. A. Tout, and O. R. Pols, *Mon. Not. R. Astron. Soc* **329**, 897 (2002).
- [48] S. Chatterjee, J. M. Fregeau, S. Umbreit, and F. A. Rasio, *The Astrophysical Journal* **719**, 915 (2010).
- [49] M. Morscher, S. Umbreit, W. M. Farr, and F. A. Rasio, *The Astrophysical Journal* **763**, L15 (2013).
- [50] J. M. Fregeau, P. Cheung, S. F. Portegies Zwart, and F. A. Rasio, *Mon. Not. R. Astron. Soc* **352**, 1 (2004).
- [51] J. M. Fregeau and F. A. Rasio, *The Astrophysical Journal* **658**, 1047 (2007).
- [52] C. L. Rodriguez, M. Morscher, L. Wang, S. Chatterjee, F. A. Rasio, and R. Spurzem, *Mon. Not. R. Astron. Soc* **463**, 2109 (2016).
- [53] L. Wang, R. Spurzem, S. Aarseth, M. Giersz, A. Askar, P. Berczik, T. Naab, R. Schadow, and M. B. N. Kouwenhoven, *Mon. Not. R. Astron. Soc* **458**, 1450 (2016).
- [54] J. S. Vink, A. de Koter, and H. J. G. L. M. Lamers, *Astronomy and Astrophysics* **369**, 574 (2001).
- [55] K. Belczynski, T. Bulik, C. L. Fryer, A. Ruiters, F. Valsecchi, J. S. Vink, and J. R. Hurley, *The Astrophysical Journal* **714**, 1217 (2010).
- [56] C. L. Fryer, K. Belczynski, G. Wiktorowicz, M. Dominik, V. Kalogera, and D. E. Holz, *The Astrophysical Journal* **749**, 91 (2012).
- [57] J. M. Antognini, B. J. Shappee, T. A. Thompson, and P. Amaro-Seoane, *Mon. Not. R. Astron. Soc* **439**, 1079 (2014).
- [58] P. Peters, *Physical Review* **136**, B1224 (1964).
- [59] D. Merritt, M. Milosavljević, M. Favata, S. A. Hughes, and D. E. Holz, *The Astrophysical Journal* **607**, L9 (2004).
- [60] E. Berti, V. Cardoso, J. A. Gonzalez, U. Sperhake, M. Hannam, S. Husa, and B. Brügmann, *Physical Review D* **76**, 064034 (2007).
- [61] M. Campanelli, C. Lousto, Y. Zlochower, and D. Merritt, *The Astrophysical Journal* **659**, L5 (2007).
- [62] J. A. González, U. Sperhake, B. Brügmann, M. Hannam, and S. Husa, *Physical Review Letters* **98**, 091101 (2007).
- [63] M. Kesden, *Physical Review D - Particles, Fields, Gravitation and Cosmology* **78**, 084030 (2008).
- [64] W. Tichy and P. Marronetti, *Physical Review D* **78**, 081501 (2008).
- [65] A. Buonanno, L. E. Kidder, and L. Lehner, *Physical Review D* **77**, 026004 (2008).
- [66] L. Rezzolla, E. Barausse, E. N. Dorband, D. Pollney, C. Reisswig, J. Seiler, and S. Husa, *Physical Review D* **78**, 044002 (2008).
- [67] C. O. Lousto and Y. Zlochower, *Physical Review D* **77**, 044028 (2008).
- [68] E. Barausse and L. Rezzolla, *The Astrophysical Journal* **704**, L40 (2009).
- [69] E. Barausse, V. Morozova, and L. Rezzolla, *The Astrophysical Journal* **758**, 63 (2012).
- [70] C. O. Lousto, Y. Zlochower, M. Dotti, and M. Volonteri, *Physical Review D* **85**, 084015 (2012).
- [71] C. O. Lousto and Y. Zlochower, *Physical Review D* **87**, 084027 (2013).
- [72] C. O. Lousto and Y. Zlochower, *Physical Review D* **89**, 104052 (2014).
- [73] K. Belczynski, A. Heger, W. Gladysz, A. J. Ruiters, S. Woosley, G. Wiktorowicz, H.-Y. Chen, T. Bulik, R. OShaughnessy, D. E. Holz, et al., *Astronomy & Astrophysics* **594**, A97 (2016).
- [74] M. Fishbach and D. E. Holz *The Astrophysical Journal* **851**, L25 (2017).
- [75] C. L. Rodriguez, C.-J. Haster, S. Chatterjee, V. Kalogera, and F. A. Rasio, *The Astrophysical Journal* **824**, L8 (2016).
- [76] J. Samsing and E. Ramirez-Ruiz, *The Astrophysical Journal Letters* **840**, L14 (2017).
- [77] J. Samsing (2017), arXiv: astro-ph/1711.07452.
- [78] M. Morscher, B. Pattabiraman, C. Rodriguez, F. A. Rasio, and S. Umbreit, *The Astrophysical Journal* **800**, 9 (2015).
- [79] D. C. Heggie, *Mon. Not. R. Astron. Soc* **173**, 729 (1975).
- [80] M. J. Benacquista and J. M. B. Downing, *Living Reviews in Relativity* **16**, 4 (2013), 1110.4423.
- [81] B. P. Abbott, R. Abbott, T. D. Abbott, M. R. Abernathy, F. Acernese, K. Ackley, C. Adams, T. Adams, P. Addesso, R. X. Adhikari, et al., *Living Rev Relativ* **19**, 1 (2016), 1304.0670.
- [82] H.-Y. Chen, D. E. Holz, J. Miller, M. Evans, S. Vitale,

- and J. Creighton (2017), arXiv: astro-ph/1709.08079.
- [83] M. C. Miller and J. M. Miller, *Physics Reports* **548**, 1 (2015).
- [84] M. Campanelli, C. Lousto, Y. Zlochower, and D. Merritt, *The Astrophysical Journal* **659**, L5 (2007).
- [85] C. O. Lousto, H. Nakano, Y. Zlochower, and M. Campanelli, *Phys Rev D* **81** (2010), 0910.3197.
- [86] S. Vitale, R. Lynch, J. Veitch, V. Raymond, and R. Sturani, *Physical Review Letters* **112**, 251101 (2014), 1403.0129.
- [87] L. Blanchet, *Living Reviews in Relativity* **9**, 4 (2006).
- [88] D. Gerosa and M. Kesden, *Physical Review D* **93**, 124066 (2016).
- [89] A. Askar, M. Szkudlarek, D. Gondek-Rosińska, M. Giersz, and T. Bulik, *Mon. Not. R. Astron. Soc. Lett.* **464**, L36 (2016).
- [90] F. Antonini and F. A. Rasio, *The Astrophysical Journal* **831**, 187 (2016), 1606.04889.
- [91] M. Giesler, D. Clausen, and C. D. Ott (2017), arXiv: astro-ph/1708.05915.
- [92] L. Wen, *The Astrophysical Journal* **598**, 419 (2003).
- [93] I. R. King, *The Astronomical Journal* **71**, 64 (1966).
- [94] P. Kroupa, *Mon. Not. R. Astron. Soc* **322**, 231 (2001).
- [95] M. Spera and M. Mapelli, *Mon. Not. R. Astron. Soc* **4**, 4739 (2017).

Appendix A: Post-Newtonian Physics

Our post-Newtonian (pN) scattering code was originally presented in detail in [27, 57], building upon the well-tested and commonly used `fewbody` code [50]. `fewbody` computes strong binary-single and binary-binary encounters using an 8th-order RungeKutta Prince-Dormand integrator. Because the pN corrections to the equations of motion can be expressed in terms of pair-wise position- and velocity-dependent accelerations [see e.g., 87], these terms are easily incorporated into `fewbody`. To incorporate both conservative and dissipative relativistic effects (i.e., GW emission), the pN force terms are included in the code up to 3.5pN order, though for the current study we only use the 1pN, 2pN, and 2.5pN terms. This code has been shown to conserve energy when dissipative effects are ignored, and to reproduce accurately the inspiral times predicted by [58]. See Appendices A1 and A2 in [57].

We detect a merger of two BHs in `fewbody` using a standard sticky-sphere collision criterion where the effective radii of the BHs are set to 5 Schwarzschild radii ($10Gm/c^2$). Any two BHs touching within these radii are assumed to merge. For BBH mergers that occur during a `fewbody` integration, we determine the final mass, spin, and recoil kick of the merger remnant using the fitting formulas compiled in [88], based on extensive work by [59–72]. Due to a typo in the original published version, we reproduce the correct formula for the final mass here, while referring the reader to [88] for the prescriptions for the final spin and recoil kick. For the final mass, we use the interpolated fit between the test-particle limits [63] and numerical relativity [60, 72] that was given in [68].

This equation is incorrect in [88], and should read

$$\frac{M_f}{M} = 1 - \eta(1 - 4\eta)(1 - E_{\text{ISCO}}) - 16\eta^2 [p_0 + 4p_1\tilde{\chi}_{\parallel}(\tilde{\chi}_{\parallel} + 1)] \quad (\text{A1})$$

where M_f/M is the ratio of the remnant mass to the binary mass, $\eta \equiv m_1 m_2 / (m_1 + m_2)^2$, $p_0 = 0.04827$, $p_1 = 0.01707$ [from 68] and E_{ISCO} is the energy at the innermost-stable-circular orbit for a Kerr BH:

$$E_{\text{ISCO}} = \sqrt{1 - \frac{2}{3r_{\text{ISCO}}}} \quad (\text{A2})$$

$$r_{\text{ISCO}} = 3 + Z_2 - \text{sign}(\tilde{\chi}_{\parallel})\sqrt{(3 - Z_1)(3 + Z_1 + 2Z_2)} \quad (\text{A3})$$

$$Z_1 \equiv 1 + (1 - \tilde{\chi}_{\parallel}^2)^{1/3} \left[(1 + \tilde{\chi}_{\parallel})^{1/3} + (1 - \tilde{\chi}_{\parallel})^{1/3} \right] \quad (\text{A4})$$

$$Z_2 \equiv \sqrt{3\tilde{\chi}_{\parallel}^2 + Z_1^2} \quad (\text{A5})$$

and where $\tilde{\chi}_{\parallel}$ is:

$$\tilde{\chi}_{\parallel} \equiv \left[\frac{m_1^2 \vec{\chi}_1 + m_2^2 \vec{\chi}_2}{(m_1 + m_2)^2} \right] \cdot \hat{L} \quad (\text{A6})$$

Note that $\tilde{\chi}_{\parallel}$ is not the same as χ_{eff} in equation (1). We track the spin magnitudes of any BHs during the integration, while for mergers, the spin directions (needed for the computation of the product mass, spin, and kick) are assumed to be isotropically distributed on the sphere. The recoil kick from [84] is decomposed into a component perpendicular to the orbital angular momentum (to which both an asymmetric mass ratio and the spins will contribute) and a component parallel to the angular momentum, which arises only from the spins. We draw a random angle in the plane of the binary for the perpendicular component and apply the two kicks in this coordinate frame.

During integrations of three- and four-body encounters, we do not stop the integration when two BHs merge, but instead continue until `fewbody`'s standard termination criteria (which check for unbound collections of objects and dynamical stability) are satisfied. This allows us to self-consistently track the outcome of mergers during dynamical encounters, which can be important for the retention of BH merger products.

For BH – (non BH) star mergers, we do not consider any accretion of material from the star, and assume that the entire star is tidally disrupted. This is a highly-conservative assumption, but is safest without a better treatment for accretion and spin-up of compact objects (which, while potentially interesting, is beyond the scope of this study).

For isolated BBHs in the cluster, CMC had previously relied on BSE to determine the change in eccentricity (e) and semi-major axis (a) at each timestep. However, the

evolution of a and e , when averaged over the binary orbit, depends strongly on the eccentricity [58]:

$$\left\langle \frac{da}{dt} \right\rangle = -\frac{64}{5} \frac{G^3 m_1 m_2 (m_1 + m_2)}{c^5 a^3 (1 - e^2)^{7/2}} \left(1 + \frac{73}{24} e^2 + \frac{37}{96} e^4 \right) \quad (\text{A7})$$

$$\left\langle \frac{de}{dt} \right\rangle = -\frac{304}{15} e \frac{G^3 m_1 m_2 (m_1 + m_2)}{c^5 a^4 (1 - e^2)^{5/2}} \left(1 + \frac{121}{304} e^2 \right) \quad (\text{A8})$$

As BSE uses a forward-Euler integration for its equations, it can underestimate the merger time for binaries that reach very high eccentricities. As an example, BSE will overestimate the merger time of a $30M_\odot + 30M_\odot$ binary with a semi-major axis of 0.1 AU and an eccentricity of 0.9 by nearly 20%. Furthermore, by default, BSE only applies GW energy loss to binaries with $a < 10R_\odot$. This assumption leads BSE to *significantly* underestimate the number of GW-driven mergers for binaries in a typical cluster, which can be highly eccentric and very massive. When accounting for GW energy loss, the number of in-cluster mergers becomes comparable to the number of mergers that are ejected from the cluster, as stated in the main text. This result represents a significant departure from previous dynamical results in the literature [15, 20, 75, 89], where ejected BBHs dominated the merger rate in the local universe. Alternative semi-analytic techniques [e.g., 90, 91] have reported significantly higher fractions of in-cluster mergers, similar to those presented here.

For isolated binaries in the cluster, we directly integrate equations (A7) and (A8) using an 8th-order Runge-Kutta Prince-Dormand integrator. This is done outside of the BSE package, so that any merging binaries use the same final mass, final spin, and recoil fitting-formula that are employed for mergers in the `fewbody` integrator. As with mergers occurring during encounters, we terminate the integration when the effective radii of the two BHs (5 Schwarzschild radii) touch. To determine the eccentricity for these systems in Figure 1, we integrate de/da , found by dividing equations (A7) and (A8). We integrate from the last-reported a and e in the cluster for each binary (which, for mergers in `fewbody`, is the a and e at the point of contact) to the semi-major axis corresponding to a circular GW frequency $f_{\text{GW}} = 10$ Hz (where $f_{\text{GW}} = 2f_{\text{orbital}}$). Although fitting formulae exist for the peak GW frequency of eccentric mergers [e.g., 92], we do not use these here, as several of these GW-capture BBHs form *inside* the LIGO/Virgo band, and therefore did not pass through the eccentric 10Hz threshold as an isolated binary.

Appendix B: GC Models

We evolve a 4x3x2 grid of GC models with different initial masses, metallicities (assumed correlated with galactocentric distance), and virial radii. These clusters

have identical initial conditions to those considered and discussed in more detail in [21]. We consider clusters with 2×10^5 , 5×10^5 , 10^6 , and 2×10^6 particles (single or binary stars) initially, covering a realistic range of GC masses. The initial positions and velocities are distributed in phase space following a standard King model [93] with concentration $W_0 = 5$. The virial radii of the clusters are then scaled to 1 or 2 pc, representing a realistic range of initial sizes. The individual stellar masses are drawn from the range $0.08 M_\odot$ to $150 M_\odot$ assuming a Kroupa initial-mass function (IMF) [94]:

$$P(m)dm \propto m^{-\alpha} dm \quad (\text{B1})$$

where

$$\alpha = \begin{cases} 1.3 & 0.08M_\odot \leq M < 0.5M_\odot \\ 2.3 & 0.5M_\odot \leq M. \end{cases} \quad (\text{B2})$$

As in our previous work we consider metallicities Z and galactocentric distances R_g of $Z = 0.005/R_g = 2$ kpc, $Z = 0.001/R_g = 8$ kpc, and $Z = 0.0002/R_g = 20$ kpc, following the correlation of metallicities with distance observed for GCs in the Milky Way. Finally, we select 10% of particles to be binaries with separations consistent with Öpek's law (flat in $\log(a)$ from the point of stellar contact to the hard-soft boundary, where the orbital velocity equals the typical velocity of particles in the cluster) and thermal eccentricities ($p(e)de = 2e de$). The primary masses are drawn from the IMF, while the secondary masses are drawn from a uniform distribution, $m_2 \in U[0, m_1]$.

Our stellar evolution prescriptions are almost identical to those adopted in [21]. We have added new physics describing mass loss from pulsational pair instabilities and pair-instability supernovae. Briefly, we follow [73], and assume that any star whose pre-explosion helium core mass is between $45 M_\odot$ and $65 M_\odot$ will undergo pulsations that eject a significant amount of mass, until the final product is at most $45 M_\odot$. This yields a BH with a mass of $40.5 M_\odot$, assuming that 10% of the baryonic mass is lost to neutrinos during collapse. Stars with He core masses above $65 M_\odot$ are completely destroyed in pair-instability supernovae. There are significant uncertainties on these numbers, and $40 M_\odot$ is likely a conservative limit (with many studies suggesting $\sim 50 M_\odot$ for the lower limit of the mass gap [e.g., 28, 95]). However, our results here are insensitive to the specific limit adopted for stellar-mass BH remnants. BHs in GCs will always undergo mass segregation and form binaries from the most massive BHs first, regardless of how large their masses are. Furthermore, the GW recoil kicks applied to merging BBHs are independent of the total mass (depending only on the mass ratio), implying that the retention of merger products also does not depend on the total mass.